

Optimization over Trained Neural Networks: Going Large with Gradient-Based Algorithms

Jiatai Tong¹, Yilin Zhu², Thiago Serra², and Samuel Burer²

¹ Northwestern University, Evanston IL, United States

jataitong2026@u.northwestern.edu

² University of Iowa, Iowa City IA, United States

{yilin-zhu,thiago-serra,samuel-burer}@uiowa.edu

Abstract. When optimizing a nonlinear objective, one can employ a neural network as a surrogate for the nonlinear function. However, the resulting optimization model can be time-consuming to solve globally with exact methods. As a result, local search that exploits the neural-network structure has been employed to find good solutions within a reasonable time limit. For such methods, a lower per-iteration cost is advantageous when solving larger models. The contribution of this paper is two-fold. First, we propose a gradient-based algorithm with lower per-iteration cost than existing methods. Second, we further adapt this algorithm to exploit the piecewise-linear structure of neural networks that use Rectified Linear Units (ReLUs). In line with prior research, our methods become competitive with—and then dominant over—other local search methods as the optimization models become larger.

Keywords: Constraining learning · Gradient ascent · Linear regions · Piecewise-linear functions · Rectified linear units.

1 Introduction

In the field of mathematical programming, piecewise-linear functions play an important role in modeling nonlinear functions [43,41,70,45,31]. In deep learning, a popular model that provides a piecewise-linear approximation of a nonlinear function is the neural network with the ReLU activation function [2,30]. Researchers have long known that some neural network architectures are universal function approximators [13,21,28], and in particular, this is also true of the ReLU activation function if the architecture is sufficiently wide [75] or deep [26]. When neural-network approximations are used as surrogates for solving nonlinear optimization problems, algorithms that exploit the piecewise-linear structure of the neural networks are of particular interest. In this paper, we propose gradient-based algorithms for this setting.

Optimizing a piecewise-linear function over a polyhedron can be modeled using a Mixed-Integer Linear Programming (MILP) formulation. In the specific case of ReLU networks, existing MILP formulations either have a weak linear relaxation due to big M coefficients [20] or become prohibitively large when

using a disjunctive formulation [29]. Researchers have found success by improving the big M coefficients [12,20,22,36,66,3,76,27,61], strengthening formulations using valid inequalities [1], and using a hybrid of both formulations [66]. Other improvements include reformulation [29,55,38], parameter rescaling [50], pruning the search space by inference [64,73,6,56], and working with sparser neural networks [54,73,8,49].

There also exist local search methods, which do not solve the full MILPs exactly, but instead are designed to find good solutions in limited time. Indeed, the works by Perakis & Tsiourvas [48] and Tong et al. [65] are closely related to this paper. Both take a geometric view of the input space of the ReLU network, focusing on the linear pieces of the function approximation. Known as *linear regions* in machine learning, each piece corresponds to a polyhedron associated with a distinct set of active neurons. Within a linear region, changes to the input have a linear impact on the output. In Figure 1, we illustrate these concepts on a neural network having inputs x_1 and x_2 , neurons with outputs h_1 to h_5 , and output y .

We summarize the works [48,65] just mentioned, taking the liberty to name them *MILP Walk* and *LP Walk*, respectively, in order to draw parallels between these methods and our methods introduced in Section 3:

- **MILP Walk:** Perakis & Tsiourvas [48] solve a sequence of restricted MILP models. Each MILP model finds the best solution across all linear regions containing the current solution. If a better solution is found, the same process is repeated from the new solution. In Figure 2 Left, solution A lies only in the linear region in darkest gray, in which the best solution is B . In turn, solution B lies in the four linear regions with the three darker tones of gray, where the best solution is C . Finally, solution C lies in the four linear regions with the two lighter tones of gray, where the best solution is C again. Once no improvement is found, the algorithm stops.
- **LP Walk:** Tong et al. [65] solve a sequence of LP models. Each LP model finds the best solution in a linear region containing the current solution. If a better solution is found, they repeat the process by moving slightly past the new solution along the line from the last solution. Moving slightly past avoids using a solution lying in multiple linear regions. In Figure 2 Right, the linear region of solution A is in darker gray, and its best solution is along the line from A to B . In turn, the linear region of solution B is in slightly lighter gray, and its the best solution is along the line from B to C . From C we find solution E and move towards D . From D we find solution E again. At this point, the algorithm stops.

For a broader discussion about linear regions and their nexus with mathematical optimization, we recommend the survey by Huchette et al. [30].

Which algorithm, MILP Walk or LP Walk, is best suited for a particular instance often depends on the size of that instance. Starting from the same solution, it is easy to see that MILP Walk will move next to a solution that is at least as good as the one found by LP Walk. On the other hand, each iteration of MILP Walk solves the same MILP model used to optimize over the entire neural

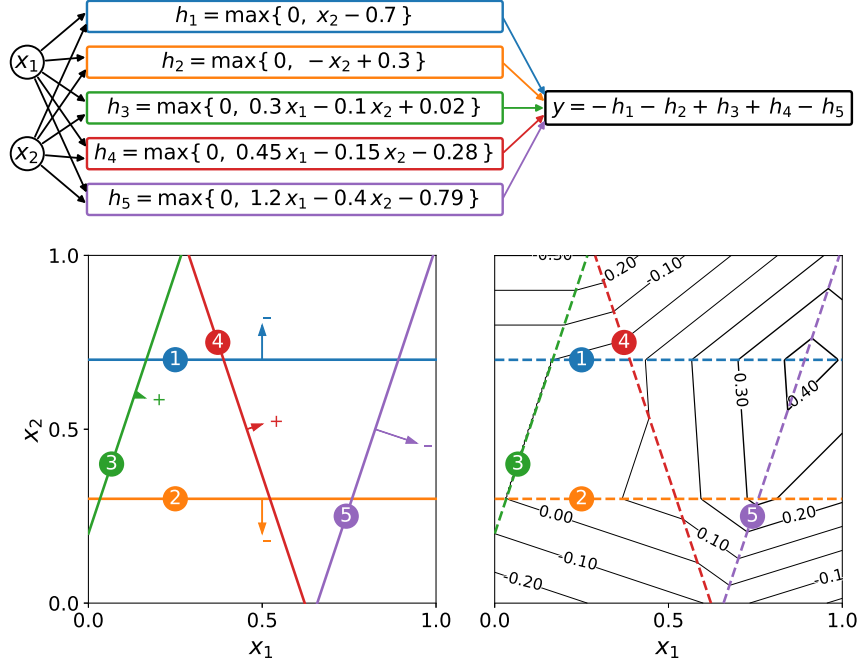


Fig. 1. Top: Visual description of neural network used as example. **Bottom left:** Lines partitioning the space based on what inputs produce a positive output for each neuron, with the arrow pointing to the positive side, the length of the arrow proportional to the magnitude of the parameters, and the arrow label denoting the influence on y . **Bottom right:** Contour plots of y over the lines associated with neural activations.

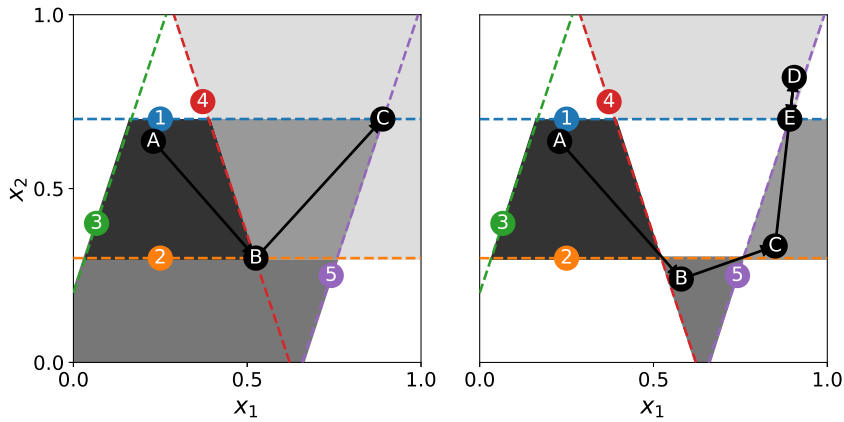


Fig. 2. Left: Solutions found by MILP Walk from the initial solution $A = (0.23, 0.636)$ until convergence. **Right:** Solutions found by LP Walk from A until convergence.

network, albeit restricted to the neighborhood of the current solution. Hence, the per-iteration cost of MILP Walk is higher than the per-iteration cost of LP Walk. Consequently, LP Walk can perform more iterations in the same amount of time. Indeed, an empirical comparison of both methods shows that LP Walk performs better for neural networks with more inputs, layers, and neurons [65], all of which imply a larger number of linear regions [57]. Thus, LP Walk conducts a style of search that is more akin to sampling than to enumeration [56].

Of course, solving an LP model for each linear region, as in LP Walk, may eventually become too costly in ever larger neural networks. Hence, in this paper, we propose a new local search approach with an even smaller per-iteration cost:

- **Gradient Walk:** We compute a sequence of gradient steps. Each step may find a better solution within the current linear region, or a solution in another linear region that is better or worse. We keep track of the best solution found. If the improvement is too small for a predefined number of steps, we restart from a perturbation of the best solution found thus far. In Figure 3 Left, we move from A to B through nine intermediary steps in the same linear region as A , all in the same direction, and then from B to C with five intermediary steps. Note that the steps are orthogonal to the contour plots within the linear regions. In Figure 3 Right, we continue from C until H by zig-zagging among linear regions and improving in all steps except G . The steps following H would not find a much better solution. Hence, the algorithm stops.

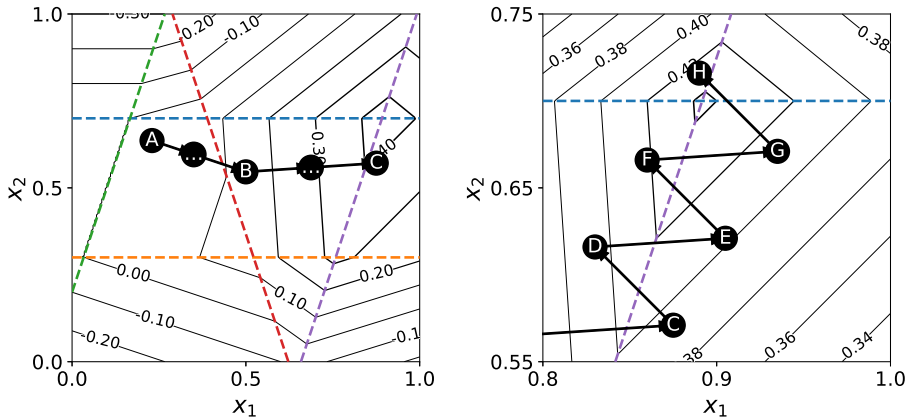


Fig. 3. **Left:** First solutions found by Gradient Walk from the initial solution $A = (0.23, 0.636)$. **Right:** Next solutions found over a narrower region of the input space.

In what follows, we define our problem of interest and its conventional MILP model in Section 2. Then we present an algorithm for Gradient Walk as well as a variant that further exploits knowledge of linear regions in Section 3. We evaluate those algorithms in Section 4. Conclusions are given in Section 5.

2 Preliminaries

We optimize the function $f : \mathbb{R}^{n_0} \rightarrow \mathbb{R}$ associated with a neural network over a polytope $\mathbb{X} \subset \mathbb{R}^{n_0}$:

$$\text{maximize}_{\mathbf{x}} \quad f(\mathbf{x}) \quad (1)$$

$$\text{s.t.} \quad \mathbf{x} \in \mathbb{X} \quad (2)$$

i.e., we want an input $\mathbf{x} = [x_1 \ x_2 \ \dots \ x_{n_0}]^\top \in \mathbb{X}$ maximizing the prediction $f(\mathbf{x})$. In the experiments of Section 4, \mathbb{X} equals a box, but our theoretical development requires only that \mathbb{X} be polyhedral.

Let the neural network have L hidden layers, each hidden layer $l \in \mathbb{L} := \{1, \dots, L\}$ having preactivation values $\mathbf{g}^l = [g_1^l \ g_2^l \ \dots \ g_{n_l}^l]^\top$ and outputs $\mathbf{h}^l = [h_1^l \ h_2^l \ \dots \ h_{n_l}^l]^\top$ from neurons indexed by $i \in \mathbb{N}_l = \{1, 2, \dots, n_l\}$. The output layer $L + 1$ has a single preactivation value g_1^{L+1} as the network output. Let \mathbf{W}^l and \mathbf{b}^l denote the weight matrix and bias vector associated with the l -th layer, for which we assume that all elements are within $[-1, 1]$. The preactivation value g_i^l of neuron i in layer l is given by $g_i^l = \mathbf{W}_i^l \mathbf{h}^{l-1} + \mathbf{b}_i^l$, and the output h_i^l of neuron i in hidden layer l follows by the ReLU activation $h_i^l = \max\{0, g_i^l\}$. In this setting, $\mathbf{x} = \mathbf{h}^0$ and $f(\mathbf{x}) = g_1^{L+1}$.

For an input $\mathbf{x} \in \mathbb{X}$, let $\mathbf{z}^l(\mathbf{x}) = [z_1^l \ z_2^l \ \dots \ z_{n_l}^l]^\top$ be the *layer activation pattern* produced in layer l of the neural network when given \mathbf{x} as input, where:

$$z_i^l = \begin{cases} 1, & \text{if } h_i^l = g_i^l \geq 0, \\ 0, & \text{if } g_i^l \leq 0. \end{cases} \quad (3)$$

A neuron is *binding* if $g_i^l = h_i^l = 0$. In this case, z_i^l can be either 0 or 1.

Let $\mathbf{z}(\mathbf{x}) = \{\mathbf{z}^1(\mathbf{x}), \mathbf{z}^2(\mathbf{x}), \dots, \mathbf{z}^L(\mathbf{x})\}$ be the *activation pattern* produced across all layers of the neural network when given \mathbf{x} as input. A *linear region* $\mathcal{R}_{\mathbf{z}'} \in \mathbb{X}$ is a set where every input \mathbf{x} has the same activation pattern \mathbf{z}' as all the other inputs, i.e., $\mathbf{z}(\mathbf{x}) = \mathbf{z}' \ \forall \mathbf{x} \in \mathcal{R}_{\mathbf{z}'}$. The output of f varies linearly within each linear region. Inputs lie in multiple linear regions if a neuron is binding.

We can formulate the optimization problem as the following MILP model:

$$\text{maximize} \quad f(\mathbf{x}) = g_1^{L+1} \quad (4)$$

$$\text{s.t.} \quad \mathbf{h}^0 = \mathbf{x}, \quad \mathbf{x} \in \mathbb{X} \quad (5)$$

$$\mathbf{W}_i^l \mathbf{h}^{l-1} + \mathbf{b}_i^l = \mathbf{g}_i^l, \quad \forall l \in \mathbb{L} \cup \{L + 1\}, i \in \mathbb{N}_l \quad (6)$$

$$(z_i^l = 1) \rightarrow (\mathbf{h}_i^l = \mathbf{g}_i^l), \quad \forall l \in \mathbb{L}, i \in \mathbb{N}_l \quad (7)$$

$$(z_i^l = 0) \rightarrow (\mathbf{g}_i^l \leq 0 \wedge \mathbf{h}_i^l = 0), \quad \forall l \in \mathbb{L}, i \in \mathbb{N}_l \quad (8)$$

$$\mathbf{h}_i^l \geq 0, \quad z_i^l \in \{0, 1\}, \quad \forall l \in \mathbb{L}, i \in \mathbb{N}_l \quad (9)$$

The indicator constraints (7)–(8) can be modeled with big M constraints [5].

We can formulate an LP model optimizing over a single linear region $\mathcal{R}_{\mathbf{z}'}$ by fixing $\mathbf{z} = \mathbf{z}'$. For example, this is what LP Walk does in each iteration.

3 Our Proposed Algorithms

We propose two gradient-based algorithms for solving (1)–(2). We assume throughout that the polyhedral domain \mathbb{X} is bounded, i.e., \mathbb{X} is a polytope. Indeed, neural networks are often used within a confined domain. There is a growing body of work on preventing a neural network from extrapolating outside the nominal or implied domain defined by a training set [60,67,77]. Moreover, the possibility of embedding a neural network as part of an MILP model depends on the input set being bounded [57], which otherwise would also prevent us from benchmarking against existing algorithms [48,65].

Our first algorithm, the Perturbed Projected Gradient Ascent (PPGA) algorithm, is described in Section 3.1. PPGA makes use of both the piecewise-constant nature of ∇f and projection onto \mathbb{X} . Our second algorithm, PPGA with Linear Region Valve (PPGA_{LR}), is described in Section 3.2. PPGA_{LR} enhances PPGA by further exploiting the structure of the linear regions, being particularly beneficial if the number of linear regions is large.

3.1 Perturbed Projected Gradient Ascent (Algorithm 1)

We first mention the standard approach, called the Projected Gradient Ascent (PGA) algorithm, of projecting the gradient steps over the feasible set to produce iterates of the form

$$\mathbf{x}^{t+1} = P_{\mathbb{X}}(\mathbf{x}^t + \gamma \nabla f(\mathbf{x}^t)), \quad (10)$$

where γ is the learning rate and L_2 projection [52,51] solves the convex quadratic program (QP)

$$P_{\mathbb{X}}(\dot{\mathbf{x}}) = \arg \min_{\mathbf{x}} \|\mathbf{x} - \dot{\mathbf{x}}\|^2 \quad (11)$$

$$\text{s.t. } \mathbf{x} \in \mathbb{X}, \quad (12)$$

which takes only $O(n_0)$ time when \mathbb{X} is a box.

Based on PGA, we now introduce our method PPGA. For any point $\mathbf{x}' \in \mathcal{R}_{\mathbf{z}(\mathbf{x})}$, i.e., any point \mathbf{x}' in the same linear region as \mathbf{x} , we can calculate $f(\mathbf{x}')$ with the affine transformation

$$f|_{\mathcal{R}_{\mathbf{z}(\mathbf{x})}}(\mathbf{x}') = T(\mathbf{z}(\mathbf{x}))\mathbf{x}' + t(\mathbf{z}(\mathbf{x})), \quad (13)$$

where

$$T(\mathbf{z}(\mathbf{x})) = \mathbf{w}^{L+1} \left(\prod_{l=1}^L (\mathbf{z}^l(\mathbf{x}) \mathbf{I}) \mathbf{W}^l \right) \quad (14)$$

and $t(\mathbf{z}(\mathbf{x}))$ is constant [30]. Hence, it follows that

$$\nabla f(\mathbf{x}) = \mathbf{w}^{L+1} \left(\prod_{l=1}^L (\mathbf{z}^l \mathbf{I}) \mathbf{W}^l \right) \quad (15)$$

for any point \mathbf{x} at the interior of its linear region, i.e., not binding for any neuron. Hence, f has a piecewise affine landscape, which may contain local maxima, saddle points, and local minima.

For smooth maximization problems, one may generally escape from (interior feasible) saddle points and local minima by introducing a perturbation when $\nabla f(\mathbf{x})$ is small enough [32,33,23,69]. Our case is quite different, however, since all differentiable regions have constant gradients and because saddle points and local minima occur at the boundary of those regions, where the function is nondifferentiable. Hence, the size of $\nabla f(\mathbf{x})$ is not a reliable measure of local optimality in our case.

We hence use a different mechanism to measure progress. If we accumulate k improvements that are relatively small in comparison to the current objective

Algorithm 1 Perturbed Projected Gradient Ascent

Input: Model f with input size n_0 , learning rate γ , time limit T , restart noise coefficient Ξ , error threshold ϵ , tolerance window k ; input domain \mathbb{X}
Output: Best solution \mathbf{x}^* and objective value $f(\mathbf{x}^*)$

```

1:  $\delta \leftarrow \frac{\Xi}{\sqrt{n_0}}$ 
2: Sample initial  $\mathbf{x} \sim \text{Uniform}(\mathbb{X})$ 
3:  $\mathbf{x}^* \leftarrow \mathbf{x}$                                  $\triangleright$  Initialized best solution so far
4:  $\mathbf{x}' \leftarrow \mathbf{x}$                              $\triangleright$  Initialized best solution since reset
5:  $r \leftarrow 0$                                      $\triangleright$  Initialized reset counter
6: while Time  $< T$  do
7:    $\mathbf{x} \leftarrow P_{\mathbb{X}}(\mathbf{x} + \gamma \nabla f(\mathbf{x}))$      $\triangleright$  Gradient step; replaced with Algorithm 2 in PPGALR
8:   if  $f(\mathbf{x}) > f(\mathbf{x}')$  then                       $\triangleright$  If found best solution since reset
9:      $\Delta \leftarrow f(\mathbf{x}) - f(\mathbf{x}')$                  $\triangleright$  Calculate local improvement before update
10:     $\mathbf{x}' \leftarrow \mathbf{x}$                              $\triangleright$  Update best solution since reset
11:    if  $f(\mathbf{x}) > f(\mathbf{x}^*)$  then                   $\triangleright$  If found best overall solution
12:       $\mathbf{x}^* \leftarrow \mathbf{x}$                              $\triangleright$  Update best overall solution
13:    end if
14:    if  $\Delta < f(\mathbf{x}) \cdot \epsilon$  then           $\triangleright$  If local improvement is below threshold
15:       $r \leftarrow r + 1$                                  $\triangleright$  Increment reset counter
16:      if  $r = k$  then                             $\triangleright$  If reached reset trigger
17:         $\mathbf{x} \leftarrow P_{\mathbb{X}}(\mathbf{x}^* + \xi)$ ,  $\xi \sim \mathcal{N}(0, \delta)$      $\triangleright$  Reset event
18:         $\mathbf{x}' \leftarrow \mathbf{x}$ 
19:         $r \leftarrow 0$ 
20:      end if
21:    else                                          $\triangleright$  If the improvement is above the threshold
22:      if  $f(\mathbf{x}) = f(\mathbf{x}^*)$  then           $\triangleright$  If current solution matches best overall
         solution
23:         $r \leftarrow 0$                                  $\triangleright$  Reset the counter
24:      end if
25:    end if
26:  end if
27: end while
28: return  $\mathbf{x}^*$ ,  $f(\mathbf{x}^*)$ 

```

value $f(\mathbf{x}^t)$, while not producing a better overall solution, then we continue the next iteration from a perturbation $\xi \sim \mathcal{N}(0, \frac{\Xi}{\sqrt{n_0}})$ around the current best solution \mathbf{x}^* . If that happens at step t , then the next update is

$$\mathbf{x}^{t+1} = P_{\mathbb{X}}(\mathbf{x}^* + \xi + \gamma \nabla f(\mathbf{x}^* + \xi)) \quad (16)$$

The resultant algorithm, our Perturbed Projected Gradient Ascent (PPGA) algorithm, is described as Algorithm 1.

3.2 PPGA With Linear Region Valve (Algorithms 1 and 2)

When the ReLU network gets deeper, the gradient calculated with Equation (15) may either explode or diminish, which makes it important to find an appropriate learning rate. As an alternative to calibrate the learning rate, we propose using linear region information for making local decisions about the size of the gradient step. Because we assume in this paper that all weights are within $[-1, 1]$, we expect the gradient to diminish when the network gets deeper. Notably, a similar approach can also be applied to resolve gradient explosion.

Suppose that we are in the linear region \mathcal{R}_z with activation pattern \mathbf{z} . We can calculate how far we may move to reach the next linear region in the direction of the gradient by a ratio test:

$$u = \min_{i \in \mathcal{I}} \left(-\frac{g_i}{\Delta g_i(\mathbf{x})} \right) \quad (17)$$

where $\mathcal{I} = \left\{ i \mid i \in \mathbb{N}_l, l \in \mathbb{L}, -\frac{g_i}{\Delta g_i(\mathbf{x})} \geq 0 \right\}$ is a subset of all neurons, and

$$\Delta g_i(\mathbf{x}) = g_i(\mathbf{x} + \nabla f(\mathbf{x})) - g_i(\mathbf{x}). \quad (18)$$

Here, u is the relative step size to the next linear region, while the actual step size is $u \cdot \|\nabla f(\mathbf{x}^t)\|$. We can use u as an estimate for the size of a linear region $\mathcal{R}_{z'}$ near \mathcal{R}_z , i.e., $\|\mathbf{z} - \mathbf{z}'\|_1 \leq \zeta$ with a relatively small ζ . Given also the relative step size γ , then we estimate the gradient step to stretch over

$$v = \left\lceil \frac{\gamma}{u} \right\rceil \quad (19)$$

linear regions around \mathcal{R}_z .

Let $V > 1$ be a predetermined valve value, which corresponds to the number of linear regions that we would like to stretch over at each gradient step. If γ is such that $v < V$ at the current linear region, then we use a scale factor c over the magnitude of the gradient:

$$\mathbf{x}^{t+1} = \begin{cases} P_{\mathbb{X}} \left(\mathbf{x}^t + c \frac{\nabla f(\mathbf{x}^t)}{\|\nabla f(\mathbf{x}^t)\|} \right), & \text{if } \gamma \leq V \cdot u, \\ P_{\mathbb{X}}(\mathbf{x}^t + \gamma \nabla f(\mathbf{x}^t)), & \text{otherwise.} \end{cases} \quad (20)$$

The adaptive gradient step replaces Line 7 in Algorithm 1 with Algorithm 2.

Algorithm 2 Adaptive Gradient Step with Linear Region Valve

Input: Current solution \mathbf{x} , learning rate γ , valve value V , scale factor c
Output: New iterate \mathbf{x}' \triangleright Replaces iterate calculated in Line 7 of Algorithm 1

- 1: $\nabla f(\mathbf{x}) \leftarrow \mathbf{w}^{L+1} \left(\prod_{l=1}^L (\mathbf{z}^l \mathbf{I}) \mathbf{W}^l \right)$
- 2: $g \leftarrow f(\mathbf{x})$
- 3: $g' \leftarrow f(\mathbf{x} + \nabla f(\mathbf{x}))$
- 4: $\Delta g \leftarrow g' - g$
- 5: $\rho \leftarrow -g/\Delta g$
- 6: Mask all negative entries in ρ with $+\infty$
- 7: $u \leftarrow \min(\rho)$
- 8: **if** $V \cdot u \geq \gamma$ **then**
- 9: $\mathbf{x}' \leftarrow P_{\mathbb{X}} \left(\mathbf{x} + c \cdot \frac{\nabla f(\mathbf{x})}{\|\nabla f(\mathbf{x})\|} \right)$
- 10: **else**
- 11: $\mathbf{x}' \leftarrow P_{\mathbb{X}}(\mathbf{x} + \gamma \cdot \nabla f(\mathbf{x}))$
- 12: **end if**
- 13: **return** \mathbf{x}'

In our implementation, we simply chose $V = \frac{1}{\|\nabla f(\mathbf{x}^t)\|}$ as an adaptive valve value, so that a small gradient will more likely trigger the rescaled gradient update. We also set $c = u$, so that we force the step size stretching more than V linear regions, since each linear region is estimated to have length $u \cdot \|\nabla f(\mathbf{x}^t)\| = \frac{u}{V}$. The main reason using adaptive hyperparameters is that applying grid search to extra hyperparameters is very costly, and we want to be fair to those algorithms with fewer hyperparameters, such as PPGA and [65].

We denote this variant of PPGA using Algorithm 2 and adaptive (V, c) design as PPGA_{LR} .

4 Numerical Experiments

We devised numerical experiments to evaluate algorithms PPGA and PPGA_{LR} on standard benchmarks and compare them with other methods. In the following subsections, we define the concept of a basic experiment, then describe our method for generating multiple experiments, and finally detail the optimization results. All numerical experiments were implemented in Python 3.10.8 using Gurobi 11.0 and evaluated on a single Xeon E5-2680v4 core running at 2.4 GHz with 16 GB of memory under the CentOS Linux operating system. The source code is publicly shared at https://github.com/yillzhu/nm_opt.

4.1 Definition of an Experiment

In our study, an *experiment* \mathcal{P} refers to a complete specification of five design options that determine the structure of a neural network and the algorithm used:

- *Input size*, i.e., the input dimension n_0 of the neural network.
- *Depth*, i.e., the number of hidden layers d of the neural network.
- *Width*, i.e., the number of neurons m in each hidden layer.
- *Seed*, i.e., the seed s used to instantiate the network parameters.
- *Algorithm*, i.e., the local search method \mathcal{M} used for optimization.

Given a particular combination of these specifications, the experiment proceeds as follows. With seed s fixed, we generate a neural network having input dimension n_0 , depth d , and width m . For each optimization algorithm \mathcal{M} , we then conduct a grid search to determine the optimal hyperparameters: shaking noise σ , error threshold ϵ , and tolerance window k . Once these parameters are fixed, the algorithm \mathcal{M} is used to optimize the network within a specified time limit.

In line with prior work [48,65] and to properly benchmark with it, we optimize over neural networks with their weights as defined at initialization. Hence, instead of optimizing over neural networks approximating specific functions based on their training, we work with neural networks representing distinct and random functions. We believe that this makes the results more representative.

4.2 Generating Multiple Experiments

In addition to PPGA and PPGA_{LR} , we use the PGA algorithm from Section 3.1 as a baseline and benchmark against the algorithm proposed for LP Walk in [65], which we denote as **SimplexWalk**. **SimplexWalk** has shown better scalability than solving directly with Gurobi [25] or with MILP Walk [48]. Hence,

$$\mathcal{M} \in \{\text{PPGA}_{\text{LR}}, \text{PPGA}, \text{PGA}, \text{SimplexWalk}\}.$$

We use input size $n_0 \in \{10, 100, 1000\}$, depth $d \in \{2, 4, 6, 8\}$, and width $m \in \{100, 1000, 10000\}$, resulting in $3 \times 3 \times 4 = 36$ distinct network configurations.

For gradient-based algorithms (PPGA_{LR} , PPGA, PGA), performance is very susceptible to hyperparameters. Therefore, we use a preprocessing phase to search for better hyperparameters for each gradient-based algorithm through grid search and voting. For each network configuration (n_0, d, m) , we generate five random networks using seeds $s \in \{5, 6, 7, 8, 9\}$. These networks, denoted as *grid search instances*, are used for choosing hyperparameters over a grid with

$$\gamma \in \{0.001, 0.01, 0.1, 1, 5\}, \quad \sigma \in \{0.2, 2, 20\}, \quad k \in \{100, 500, 1000\}.$$

For each grid search instance, we evaluate all $5 \times 3 \times 3 = 45$ parameter combinations, running the optimization for 5 minutes per grid point. The five combinations achieving the best objective values are recorded for each instance. After processing all five grid search instances, we obtain five sets of top-performing parameter combinations. The most frequently occurring combination across these sets is selected as the final grid search result for that algorithm and network configuration. This process runs independently for each gradient-based algorithm.

Once the hyperparameters are calibrated, we generate 20 additional networks for each (n_0, d, m) combination using seeds $s \in \{10, 11, \dots, 29\}$. These are referred to as *optimization instances*. Each algorithm \mathcal{M} is then applied to these

instances, and the gradient-based algorithms use the hyperparameters obtained from the grid search. Every run is executed for 7200 seconds, during which we record, at every second, the best objective value and the number of iterations.

4.3 Computational Complexity of Walk Steps

The complexity of the problem can be affected by all three setup options (n_0, d, m) . For gradient-based algorithms (PPGA_{LR} , PPGA , PGA), the asymptotic complexity of both calculating the gradient and making a prediction is

$$O(dm^2 + n_0m).$$

which can be deduced from a sequence of vector-matrix multiplications. Through Equation (18), each step of the linear region algorithm (PPGA_{LR}) may cost twice as much as PGA and PPGA steps, which we may consider still acceptable. On the other hand, **SimplexWalk** carries out the solution of one LP model per step. Notably, the computational cost of a **SimplexWalk** step, if the LP model is solved using the simplex algorithm, is exponential on n_0 in worst-case.

4.4 Results

We use the DolanMore performance profile [16,63] to compare the performance of different algorithms on multiple problems. A performance profile shows, for each algorithm, the fraction of test instances on which it performs within a given factor of the best observed result. The horizontal axis represents the performance factor $\tau \geq 1$ in log scale, and the vertical axis $\rho_{\mathcal{M}}(\tau) \in [0, 1]$ represents the fraction of experiments for which the algorithm \mathcal{M} attains a performance ratio of at most τ . The vertical intercept $\rho_{\mathcal{M}}(1)$ indicates how often an algorithm achieves the best result among all competitors, and a curve approaching $\rho = 1$ more rapidly reflects an algorithm whose performance is consistently close to the best algorithm across all experiments.

Figure 4 shows the overall performance profiles across all setups after the methods have been run for 30, 60, and 120 minutes. The other two plots focuses on the results after 120 minutes. Figure 5 shows the performance profiles from partitioning the instances according to the input size of the neural network. Figure 6 partitions the instances according to the depth and the width of the neural network.

4.5 Analysis

In general, the relationship between the three gradient algorithms is similar across different time budgets, with PPGA and PPGA_{LR} outperforming the vanilla PGA . However, the gap between the first PPGA and vanilla PGA shrinks for the largest width (10000). Since width dominates the complexity of gradient steps, it is possible that PPGA algorithms do not gain much in performance advantage in the early steps compared to the vanilla algorithm. Therefore, the advantage

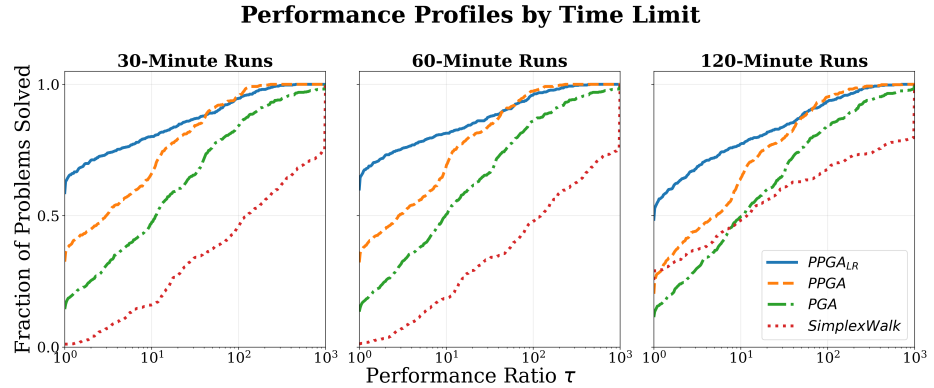


Fig. 4. Comparison of algorithm performance over all instances by varying time limit.

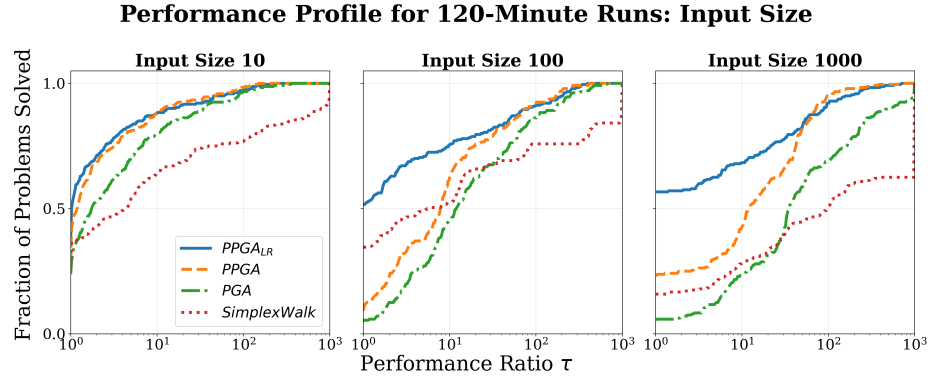


Fig. 5. Comparison of algorithm performance by varying input size in 120-minute runs.

that we observe is likely gained in the later steps, when the vanilla algorithm is captured in some local optimum while PPGA escapes through perturbation.

While PPGA_{LR} is overall better than PPGA in the aggregate of instances from Figure 4, the advantage of PPGA_{LR} is due to the instances with larger dimensions:

- From Figure 5, we see that PPGA_{LR} matches PPGA for the smallest input (10) but does significantly better than PPGA for larger input sizes (100 and 1000).
- From the rows of Figure 6, PPGA_{LR} is generally better for larger widths.
- From the columns of Figure 6, we see that PPGA_{LR} is worse for the smallest depth (2), but that it dominates the results for deeper networks (6 and 8).

Hence, larger input size and depth seem to be the most determinant factors for PPGA_{LR} performing better than PPGA. Larger width also contributes in some cases. Those conditions conform with the cases in which neural networks tend to have more linear regions, which has inspired the design of PPGA_{LR} in the first

place. Moreover, as indicated by Equation 15 and given the weight distribution, neural networks with greater depth are bound to have smaller gradients.

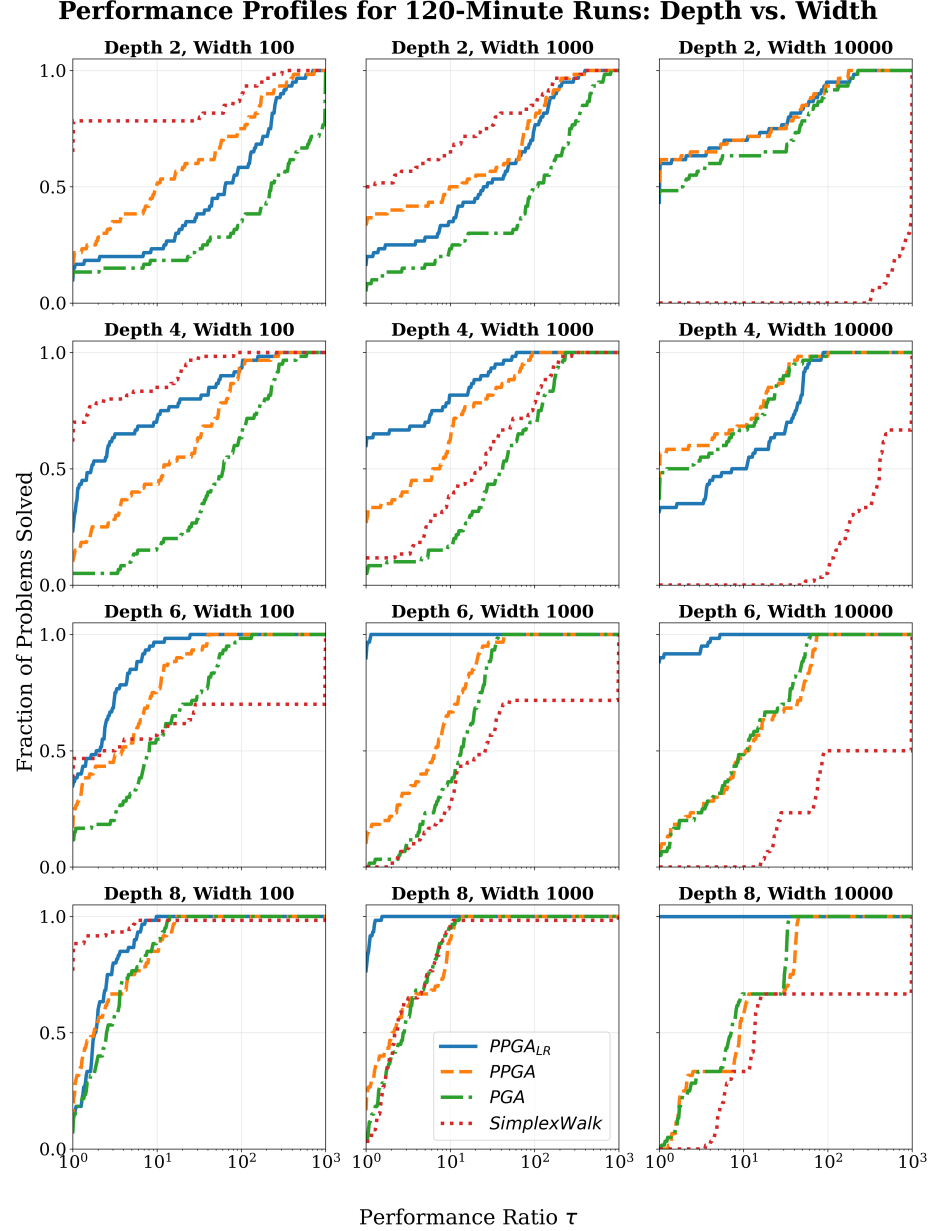


Fig. 6. Comparison of performance by varying depth and width in 120-minute runs.

Meanwhile, notably, **SimplexWalk** gets comparatively better with longer runtimes, as shown in Figure 4. That conforms with the intuition that it takes longer to converge due to the more costly steps, but that each step tends to provide greater improvements. Indeed, we observe **SimplexWalk** dominating in the three scenarios with smallest depth and width in Figure 6.

4.6 A Case Study on Adaptive Stepsize for PPGA_{LR}

To better understand why PPGA_{LR} dominates in deeper instances, we present a case study on a randomly generated instance with $(n_0 = 1000, d = 6, w = 1000)$ and seed $s = 30$. We ran 1000 iterations of PPGA with five learning rates, $\gamma \in \{5, 50, 500, 5000, 50000\}$. We also ran 1000 iterations of PPGA_{LR}, but with only three different learning rates, $\gamma \in \{5, 500, 50000\}$. We use fewer learning rates with PPGA_{LR} because there is a greater overlap in step sizes and objective values across learning rates in this case, making it harder to visually distinguish them. Figure 7 shows the influence of the learning rate γ on the step size over time. Figure 8 shows the influence of the learning rate γ on the solution value.

Our three main observations are the following:

- In PPGA, when we increase the learning rate γ , the step size changes proportionally. In PPGA_{LR}, on the other hand, the step size is less affected by the learning rate and only the size of the smallest steps are clipped.
- In PPGA, the range of step sizes for a specific learning rate is small. In PPGA_{LR}, on the other hand, the valve mechanism defined by Equation (20) allows for a larger range of step sizes regardless of learning rate. That seems to lead to similar convergence for step sizes in different orders of magnitude.
- Since there is no mechanism designed for avoiding excessively large step sizes, both algorithms perform similarly worse when $\gamma = 50000$. We could potentially address this by designing another valve and truncating large steps.

Hence, PPGA is more sensitive to the learning rate and does not converge well with lower learning rates ($\gamma \in \{5, 50\}$). In turn, PPGA_{LR} is more robust and converges well with lower learning rates in deep neural networks, as observed in Figure 6.

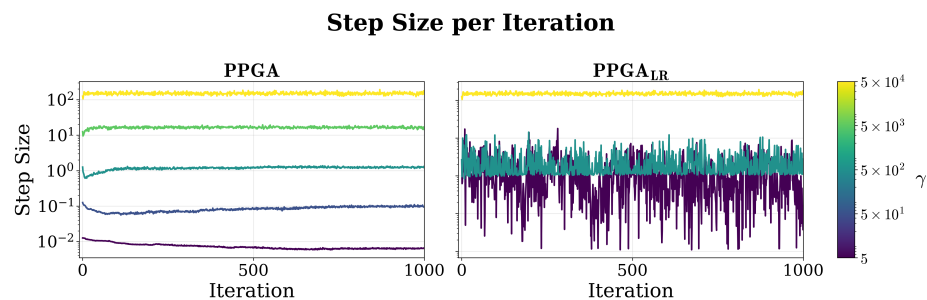


Fig. 7. Step size in log scale over iterations for PPGA (Left) and PPGA_{LR} (Right) for each learning rate.

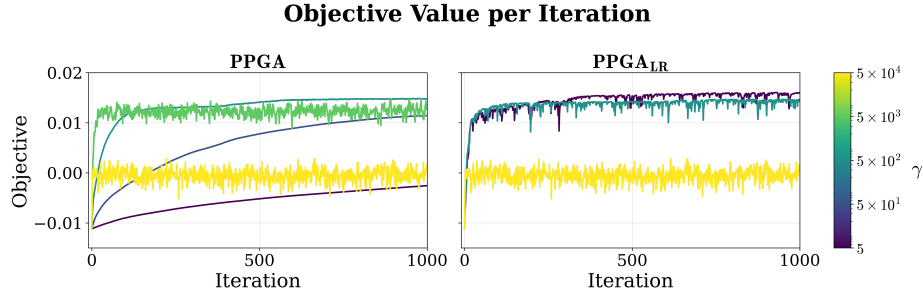


Fig. 8. Solution value over iterations for PPGA (Left) and PPGA_{LR} (Right) for each learning rate.

5 Conclusion

In this paper, we proposed Gradient Walk: a new approach for local search based on gradient steps to optimize over the piecewise affine landscape of a trained ReLU network function within a polytope. We also proposed two algorithms for this approach, PPGA and PPGA_{LR}. PPGA is based on projected gradient steps and empirically-crafted perturbations. PPGA is designed to search for a feasible solution while avoiding entrapment in arbitrary local optima constructed by the special landscape of ReLU networks. PPGA_{LR} extends PPGA by using adaptive gradient steps that stretch further when the step size is too small relative to the local affine landscape. PPGA_{LR} is designed to circumvent the issue of diminishing step sizes caused by the combination of a misaligned learning rate with small gradients observed in deep ReLU networks. We report that PPGA_{LR} has a better performance than PPGA in neural networks with larger dimensions, whereas both outperform the baseline projected gradient ascent algorithm PGA and compare favorably against the LP Walk algorithm SimplexWalk, which has previously shown better results than other alternatives in the benchmark setting [65].

In a nutshell, we double down on the trend of using specialized local search with lower per-iteration cost to find better solutions in constraint learning. We achieve that with gradient steps leveraging the local structure in ReLU networks.

Given the growing body of constraint learning applications within machine learning [1, 9, 12, 14, 17, 18, 34, 35, 37, 39, 53, 56, 57, 58, 59, 62, 67] and in mathematical optimization [4, 7, 11, 15, 38, 42, 44, 46, 47, 54, 61, 71, 72, 74], as well as the emergence of many constraint learning frameworks [4, 40, 10, 19, 42, 24, 68], the development of new algorithms to timely find better solutions is of particular importance.

In future work, we intend to devise a variant of PPGA that is also robust against large learning rates, explore how other characteristics of the landscape of ReLU networks can be leveraged to produce better algorithms, and apply the Gradient Walk approach to solve other types of constraint learning models.

Disclosure of Interests. The authors have no competing interests to declare that are relevant to the content of this article.

References

1. Anderson, R., Huchette, J., Ma, W., Tjandraatmadja, C., Vielma, J.P.: Strong mixed-integer programming formulations for trained neural networks. *Mathematical Programming* (2020)
2. Arora, R., Basu, A., Mianjy, P., Mukherjee, A.: Understanding deep neural networks with rectified linear units. In: *ICLR* (2018)
3. Badilla, F., Goycoolea, M., Muñoz, G., Serra, T.: Computational tradeoffs of optimization-based bound tightening in ReLU networks. *arXiv:2312.16699* (2023)
4. Bergman, D., Huang, T., Brooks, P., Lodi, A., Raghunathan, A.U.: JANOS: An integrated predictive and prescriptive modeling framework. *INFORMS Journal on Computing* (2022)
5. Bonami, P., Lodi, A., Tramontani, A., Wiese, S.: On mathematical programming with indicator constraints. *Mathematical Programming* (2015)
6. Botoeva, E., Kouvaros, P., Kronqvist, J., Lomuscio, A., Misener, R.: Efficient verification of (relu)-based neural networks via dependency analysis. In: *AAAI* (2020)
7. Burtea, R.A., Tsay, C.: Safe deployment of reinforcement learning using deterministic optimization over neural networks. *Computer Aided Chemical Engineering* (2023)
8. Cacciola, M., Frangioni, A., Lodi, A.: Structured pruning of neural networks for constraints learning. *Operations Research Letters* (2024)
9. Cai, J., Nguyen, K.N., Shrestha, N., Good, A., Tu, R., Yu, X., Zhe, S., Serra, T.: Getting away with more network pruning: From sparsity to geometry and linear regions. In: *CPAIOR* (2023)
10. Ceccon, F., Jalving, J., Haddad, J., Thebelt, A., Tsay, C., Laird, C.D., Misener, R.: OmLt: Optimization & machine learning toolkit. *Journal of Machine Learning Research* **23**(349), 1–8 (2022)
11. Chen, Y., Shi, Y., Zhang, B.: Data-driven optimal voltage regulation using input convex neural networks. *Electric Power Systems Research* (2020)
12. Cheng, C., Nürenberg, G., Ruess, H.: Maximum resilience of artificial neural networks. In: *ATVA* (2017)
13. Cybenko, G.: Approximation by superpositions of a sigmoidal function. *Mathematics of Control, Signals and Systems* (1989)
14. De Palma, A., Behl, H., Bunel, R.R., Torr, P., Kumar, M.P.: Scaling the convex barrier with active sets. In: *ICLR* (2021)
15. Delarue, A., Anderson, R., Tjandraatmadja, C.: Reinforcement learning with combinatorial actions: An application to vehicle routing. In: *NeurIPS* (2020)
16. Dolan, E.D., Moré, J.J.: Benchmarking optimization software with performance profiles. *Math. Program.* **91**(2), 201–213 (2002). <https://doi.org/10.1007/s101070100263>, <https://doi.org/10.1007/s101070100263>
17. Dutta, S., Jha, S., Sankaranarayanan, S., Tiwari, A.: Output range analysis for deep feedforward networks. In: *NFM* (2018)
18. ElAraby, M., Wolf, G., Carvalho, M.: OAMIP: Optimizing ANN architectures using mixed-integer programming. In: *CPAIOR* (2023)
19. Fajemisin, A., Maragno, D., den Hertog, D.: Optimization with constraint learning: A framework and survey. *European Journal of Operational Research* (2023)
20. Fischetti, M., Jo, J.: Deep neural networks and mixed integer linear optimization. *Constraints* (2018)
21. Funahashi, K.I.: On the approximate realization of continuous mappings by neural networks. *Neural Networks* (1989)

22. Grimstad, B., Andersson, H.: ReLU networks as surrogate models in mixed-integer linear programs. *Computers & Chemical Engineering* (2019)
23. Guo, X., Han, J., Tajrobehkar, M., Tang, W.: Escaping saddle points efficiently with occupation-time-adapted perturbations. *arXiv preprint arXiv:2005.04507* (2020)
24. Gurobi Optimization: Gurobi Machine Learning. <https://github.com/Gurobi/gurobi-machinelearning> (2025), accessed: 2025-02-09
25. Gurobi Optimization, LLC: Gurobi Optimizer Reference Manual (2024), <https://www.gurobi.com>
26. Hanin, B., Sellke, M.: Approximating continuous functions by ReLU nets of minimal width. *arXiv:1710.11278* (2017)
27. Hojny, C., Zhang, S., Campos, J.S., Misener, R.: Verifying message-passing neural networks via topology-based bounds tightening. In: *ICML* (2024)
28. Hornik, K., Stinchcombe, M., White, H.: Multilayer feedforward networks are universal approximators. *Neural Networks* (1989)
29. Huchette, J.: Advanced mixed-integer programming formulations: Methodology, computation, and application. Ph.D. thesis, Massachusetts Institute of Technology (2018)
30. Huchette, J., Muñoz, G., Serra, T., Tsay, C.: When deep learning meets polyhedral theory: A survey. *arXiv:2305.00241* (2023)
31. Huchette, J., Vielma, J.P.: Nonconvex piecewise linear functions: Advanced formulations and simple modeling tools. *Operations Research* (2023)
32. Jin, C., Ge, R., Netrapalli, P., Kakade, S.M., Jordan, M.I.: How to escape saddle points efficiently. In: *International conference on machine learning*. pp. 1724–1732. *PMLR* (2017)
33. Jin, C., Netrapalli, P., Jordan, M.I.: Accelerated gradient descent escapes saddle points faster than gradient descent. In: *Conference On Learning Theory*. pp. 1042–1085. *PMLR* (2018)
34. Kanamori, K., Takagi, T., Kobayashi, K., Ike, Y., Uemura, K., Arimura, H.: Ordered counterfactual explanation by mixed-integer linear optimization. In: *AAAI* (2021)
35. Kumar, A., Serra, T., Ramalingam, S.: Equivalent and approximate transformations of deep neural networks. *arXiv:1905.11428* (2019)
36. Liu, C., Arnon, T., Lazarus, C., Strong, C., Barrett, C., Kochenderfer, M.J., et al.: Algorithms for verifying deep neural networks. *Foundations and Trends® in Optimization* (2021)
37. Liu, X., Han, X., Zhang, N., Liu, Q.: Certified monotonic neural networks. In: *NeurIPS*. vol. 33 (2020)
38. Liu, X., Dvorkin, V.: Optimization over trained neural networks: Difference-of-convex algorithm and application to data center scheduling. *IEEE Control Systems Letters* (2025)
39. Lomuscio, A., Maganti, L.: An approach to reachability analysis for feed-forward ReLU neural networks. *arXiv:1706.07351* (2017)
40. Lueg, L., Grimstad, B., Mitsos, A., Schweidtmann, A.M.: reluMIP: Open source tool for MILP optimization of relu neural networks (2021). <https://doi.org/https://doi.org/10.5281/zenodo.5601907>, https://github.com/ChemEngAI/ReLU_ANN_MILP
41. Mangasarian, O.L., Rosen, J.B., Thompson, M.E.: Global minimization via piecewise-linear underestimation. *Journal of Global Optimization* (2005)
42. Maragno, D., Wiberg, H., Bertsimas, D., Birbil, S.I., Hertog, D.d., Fajemisin, A.: Mixed-integer optimization with constraint learning. *Operations Research* (2023)

43. McCormick, G.P.: Computability of global solutions to factorable nonconvex programs: Part I convex underestimating problems. *Mathematical Programming* (1976)
44. McDonald, T., Tsay, C., Schweidtmann, A.M., Yorke-Smith, N.: Mixed-integer optimisation of graph neural networks for computer-aided molecular design. *Computers & Chemical Engineering* (2024)
45. Misener, R., Floudas, C.A.: Piecewise-linear approximations of multidimensional functions. *Journal of Optimization Theory and Applications* (2010)
46. Misener, R., Biegler, L.: Formulating data-driven surrogate models for process optimization. *Computers & Chemical Engineering* (2023)
47. Murzakhanov, I., Venzke, A., Misyris, G.S., Chatzivasileiadis, S.: Neural networks for encoding dynamic security-constrained optimal power flow. In: *Bulk Power Systems Dynamics and Control Symposium* (2022)
48. Perakis, G., Tsiorvas, A.: Optimizing objective functions from trained relu neural networks via sampling. *arXiv:2205.14189* (2022)
49. Pham, H., Ren, A., Tahir, I., Tong, J., Serra, T.: Optimization over trained (and sparse) neural networks: A surrogate within a surrogate. *arXiv:2505.01985* (2025)
50. Plate, C., Hahn, M., Klimek, A., Ganzer, C., Sundmacher, K., Sager, S.: An analysis of optimization problems involving ReLU neural networks. *arXiv:2502.03016* (2025)
51. Polyak, B.T., Levitin, E.: Constrained minimization methods. *USSR Computational Mathematics and Mathematical Physics* **6** 5, 1–50 (1966)
52. Rosen, J.B.: The gradient projection method for nonlinear programming. part i. linear constraints. *Journal of the society for industrial and applied mathematics* **8**(1), 181–217 (1960)
53. Rössig, A., Petkovic, M.: Advances in verification of ReLU neural networks. *Journal of Global Optimization* (2021)
54. Say, B., Wu, G., Zhou, Y.Q., Sanner, S.: Nonlinear hybrid planning with deep net learned transition models and mixed-integer linear programming. In: *IJCAI* (2017)
55. Schweidtmann, A.M., Mitsos, A.: Deterministic global optimization with artificial neural networks embedded. *Journal of Optimization Theory and Applications* (2019)
56. Serra, T., Ramalingam, S.: Empirical bounds on linear regions of deep rectifier networks. In: *AAAI* (2020)
57. Serra, T., Tjandraatmadja, C., Ramalingam, S.: Bounding and counting linear regions of deep neural networks. In: *ICML* (2018)
58. Serra, T., Yu, X., Kumar, A., Ramalingam, S.: Scaling up exact neural network compression by ReLU stability. In: *NeurIPS* (2021)
59. Serra, T., Kumar, A., Ramalingam, S.: Lossless compression of deep neural networks. In: *CPAIOR* (2020)
60. Shi, C., Emadikhiav, M., Lozano, L., Bergman, D.: Constraint learning to define trust regions in optimization over pre-trained predictive models. *INFORMS Journal on Computing* (2024)
61. Sosnin, P., Tsay, C.: Scaling mixed-integer programming for certification of neural network controllers using bounds tightening. In: *CDC* (2024)
62. Strong, C.A., Wu, H., Zeljić, A., Julian, K.D., Katz, G., Barrett, C., Kochenderfer, M.J.: Global optimization of objective functions represented by ReLU networks. *Machine Learning* (2021)
63. Tits, A.L., Yang, Y.: Globally convergent algorithms for robust pole assignment by state feedback. *IEEE Trans. Automat. Control* **41**(10), 1432–1452 (1996). <https://doi.org/10.1109/9.539425>, <https://doi.org/10.1109/9.539425>

64. Tjeng, V., Xiao, K., Tedrake, R.: Evaluating robustness of neural networks with mixed integer programming. In: ICLR (2019)
65. Tong, J., Cai, J., Serra, T.: Optimization over trained neural networks: Taking a relaxing walk. In: International Conference on the Integration of Constraint Programming, Artificial Intelligence, and Operations Research. pp. 221–233. Springer (2024)
66. Tsay, C., Kronqvist, J., Thebel, A., Misener, R.: Partition-based formulations for mixed-integer optimization of trained ReLU neural networks. In: NeurIPS (2021)
67. Tsourvas, A., Sun, W., Perakis, G.: Manifold-aligned counterfactual explanations for neural networks. In: AISTATS (2024)
68. Turner, M., Chmiela, A., Koch, T., Winkler, M.: PySCIPOpt-ML: Embedding trained machine learning models into mixed-integer programs. In: CPAIOR (2020)
69. Vahedi, A.M., Ilies, H.T.: Spgd: Steepest perturbed gradient descent optimization. arXiv preprint arXiv:2411.04946 (2024)
70. Vielma, J.P., Ahmed, S., Nemhauser, G.: Mixed-integer models for nonseparable piecewise-linear optimization: Unifying framework and extensions. Operations Research (2010)
71. Wang, K., Lozano, L., Cardonha, C., Bergman, D.: Optimizing over an ensemble of trained neural networks. INFORMS Journal on Computing (2023)
72. Wu, G., Say, B., Sanner, S.: Scalable planning with deep neural network learned transition models. Journal of Artificial Intelligence Research (2020)
73. Xiao, K.Y., Tjeng, V., Shafiqullah, N.M., Madry, A.: Training for faster adversarial robustness verification via inducing ReLU stability. In: ICLR (2019)
74. Yang, S., Bequette, B.W.: Optimization-based control using input convex neural networks. Computers & Chemical Engineering (2021)
75. Yarotsky, D.: Error bounds for approximations with deep ReLU networks. Neural Networks (2017)
76. Zhao, H., Hijazi, H., Jones, H., Moore, J., Tanneau, M., Hentenryck, P.V.: Bound tightening using rolling-horizon decomposition for neural network verification. In: CPAIOR (2024)
77. Zhu, Y., Burer, S.: An extended validity domain for constraint learning. arXiv:2406.10065 (2024)